

Analytical solution for the potential distribution in a stripe Schottky contact

N. V. Vostokov^{a)} and V. I. Shashkin

Institute for Physics of Microstructures of the Russian Academy of Sciences, 603950 Nizhny Novgorod, Russia and N. I. Lobachevsky State University of Nizhny Novgorod, 603950 Nizhny Novgorod, Russia

(Received 7 May 2014; accepted 12 June 2014; published online 23 June 2014)

We consider a model of the stripe Schottky contact with a uniformly doped semiconductor. It is assumed that at the boundary of the semiconductor, the position of the Fermi level is fixed due to the high density of surface states in the band gap. An analytical solution of the problem of the potential distribution, the shape of the depletion region, and the high-frequency capacitance of the contact is found in the full depletion approximation. Based on the approach developed, we study quadratic nonlinear properties of the FET with a Schottky barrier in the high-frequency signal detection mode. © 2014 AIP Publishing LLC. [<http://dx.doi.org/10.1063/1.4885036>]

I. INTRODUCTION

The metal-semiconductor contact with a Schottky barrier is widely used in various semiconductor devices. Increasing the degree of integration and the operating frequencies of modern devices require that the lateral sizes of the planar contacts should be reduced to a value comparable to or smaller than the thickness of the depleted layer of the semiconductor. With such sizes, the shape of the potential Schottky barrier fundamentally cannot be described in terms of the one-dimensional model of a large planar contact. Edge effects become significant or even crucial for characteristics of the contact; therefore, the distribution of the potential should be found from the solution of a three-dimensional Poisson equation. The case is similar for the inhomogeneous Schottky contacts containing the sections with modified barrier height.¹ These sections can be related with the defects of the metal-semiconductor interface and may have nanometer lateral sizes.²

There are many papers devoted to the calculation of the potential and transport properties of the Schottky contacts that are limited and inhomogeneous in the lateral direction. For example, Ref. 3 is devoted to the numerical calculation of the distribution of the potential and capacitance of a planar Schottky contact with stripe geometry to a semi-infinite, uniformly doped semiconductor. The shape of the potential Schottky barrier and I - V characteristics for rounded planar contacts were numerically calculated in Ref. 4. In those papers, it was assumed that the metal-free surface of the semiconductor does not contain surface states, and its charge is equal to zero. On the actual surface of a semiconductor, the surface states are present. Their charge has an impact on the potential distribution in the contact. Usually, the surface density of states in the band gap of a semiconductor is so large that the Fermi level on its surface has a fixed position relative to the edges of the bands.¹ The results of numerical calculation of the potential distribution and I - V characteristics for planar Schottky nanocontacts of different shapes with allowance for the Fermi level pinning on the free surface of a semiconductor are given in Ref. 5. The problem of the potential distribution in a large planar Schottky contact

containing a nanometer region with modified barrier height is formulated mathematically identically. A numerical solution of this problem for the regions having the form of a stripe or a circle was obtained in Ref. 6. An approximate analytical solution was found in Ref. 7.

If the potential distribution in the device depends only on two Cartesian coordinates; then, the methods of the boundary-value problems in the theory of analytical functions are efficient. A conformal mapping technique has successfully been used for the analytical modeling of various semiconductor devices.^{8–12} In some cases, conformal mapping cannot be directly used since the shape of the boundary of the region in which the potential is sought is not known. This boundary-value problem with a free boundary was solved in Ref. 13. In that paper, an analytical solution was obtained for the potential distribution, the shape of the depletion region, and the barrier capacitance of a stripe Schottky contact, excluding the surface states at the semiconductor boundary outside the metal.

In the present paper, using the full depletion approximation, we find an exact analytical solution for the electrostatic potential distribution and shape of the depletion region in a planar Schottky contact with stripe geometry to a semi-infinite, uniformly doped semiconductor. It is assumed that at the boundary of a semiconductor, the position of the Fermi level is fixed due to the high density of surface states in the band gap. For frequencies much greater than the rate of recharge of surface states, the behavior of the Schottky contact capacitance and quadratic nonlinear properties of the FET with a Schottky barrier in the high-frequency signal detection mode are considered.

II. DISTRIBUTION OF THE ELECTROSTATIC POTENTIAL AND THE SHAPE OF THE DEPLETION REGION IN THE SCHOTTKY CONTACT

We consider the contact between a rectangular metal layer and the uniformly doped semiconductor. For definiteness, the problem is solved for an n -type semiconductor. It is assumed that at the boundary of a semiconductor, there are surface states with a high density of states, which ensure that the surface potential is constant with respect to the Fermi level. Therefore, the entire surface of the semiconductor is

^{a)}Electronic address: vostokov@ipm.sci-nnov.ru

depleted. The thickness of the depletion region is y_0 away from the metal and is y_m under the metal. The quantity y_0 is given and the quantity y_m is not known in advance. The length of the metal layer in the direction of the Ox axis is equal to a . The size of the contact in the direction of the Oz axis is much greater than all typical scales of the problem. The geometry of the Schottky contact is shown in Fig. 1. In the xOy plane, the depletion region is limited by the $ABB'DFA'$ curve. Part of the boundary AB separated the depleted and quasi-neutral regions of the semiconductor, the segment DF is a boundary with the metal, the segments $B'D$ and FA' correspond to a free surface of the semiconductor, and the points A, A', B , and B' are at infinity. In the full depletion approximation, the distribution of the electrostatic potential in the depletion region can be described by a two-dimensional Poisson equation

$$\frac{\partial^2 \varphi}{\partial x^2} + \frac{\partial^2 \varphi}{\partial y^2} = -1, \quad (1)$$

with the boundary conditions

$$(\varphi)_{AB} = 0, \quad (2)$$

$$(\varphi)_{B'D} = (\varphi)_{FA'} = -1, \quad (3)$$

$$(\varphi)_{DF} = -V_m, \quad (4)$$

$$\left(\frac{\partial \varphi}{\partial x}\right)_{x \rightarrow \pm \infty} = 0, \quad (5)$$

$$\left(\frac{\partial \varphi}{\partial n}\right)_{AB} = 0, \quad (6)$$

where n is the direction of the normal to the boundary of the depletion region. Hereafter, we use dimensionless variables related to dimensional quantities by $x, y = \tilde{x}, \tilde{y} / \sqrt{\tilde{V}_c \epsilon \epsilon_0 / q \tilde{N}}$ and $\varphi = \tilde{\varphi} / \tilde{V}_c$, where $-\tilde{V}_c$ is the surface potential of the semiconductor away from the metal. \tilde{N} is the dopant concentration, and ϵ is the relative dielectric permittivity of the semiconductor. The shape of the curve AB is not known, but two boundary conditions, (2) and (6), are specified on AB . Therefore, the problem can be reduced to the inverse mixed boundary-value problem in the theory of analytical functions.¹⁴

Following the approach given in Ref. 13, we introduce an auxiliary function $u = \varphi + y^2/2$, which is harmonic in the xOy plane, and is therefore the real part of some analytical function w_1 . Consider the function $w = dw_1/dz = \partial u / \partial x - i \partial u / \partial y$, where i is the imaginary unit and

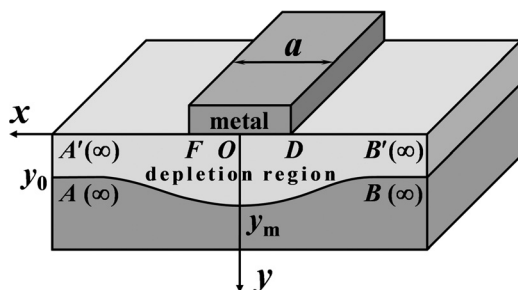


FIG. 1. Geometry of the Schottky contact.

$z = x + iy$. Using boundary conditions (2)–(6), we construct in the complex plane w a domain D_w , which corresponds to the depletion region in the complex plane z . The domain D_w is the entire complex plane w with two excluded beams on the imaginary axis. The complex plane w is shown in Fig. 2. The excluded beams are shown by dotted lines. The segments AA' and BB' degenerate into a point, and the points D and F correspond to an infinitely remote point. As a geometric parameter of the inverse problem relating the boundary values of the function w at the boundary of D_w with the boundary of the depletion region in the z plane, it is convenient to use the ordinate y . It follows from the boundary conditions that $y = -\text{Im} w$ on a part of the boundary of D_w , which corresponds to AB , and that $y = 0$ on the other part of the boundary of D_w . Since y is the real part of $-iz$, we pose the Schwarz problem¹⁴ of finding the function $-iz$, which is analytical in D_w and whose real part at the boundary of D_w takes given values. To solve the Schwarz problem, we pass from the domain D_w to a simpler region, for which an explicit expression for the Schwarz operator is known. We, then, introduce an auxiliary complex plane $\zeta = \xi + i\eta$ and find the conformal mapping, which assigns to the domain D_w the upper half-plane of the complex plane ζ . Using the Schwarz–Christoffel integral,¹⁵ we find a function to implement this mapping. This function is given by

$$w(\zeta) = -i\alpha^2(y_m - y_0) \frac{\zeta^2 - 1}{\zeta^2 - \alpha^2} - iy_0. \quad (7)$$

The boundary of the depletion region corresponds to the real axis of the complex plane ζ . The points $F, A (A'), B (B')$, and D correspond to the points $\xi = -\alpha, -1, 1$, and α , respectively. The point O corresponds to an infinitely remote point. From expression (7), it follows that the electric field tends to infinity at the edges of a metal stripe. Using the Schwarz integral for the half-plane, we find the connection between z and ζ , which has the form

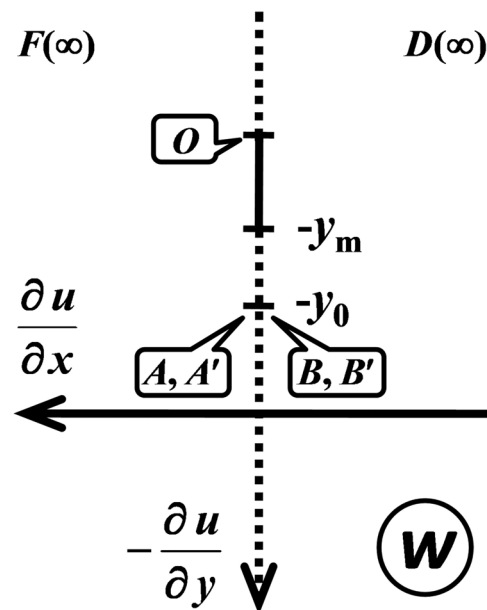


FIG. 2. Domain D_w in the complex plane w .

$$z(\zeta) = \frac{1}{\pi} \int_{-1}^{+1} \frac{\text{Im} w(\zeta, \eta=0)}{\zeta - \xi} d\xi. \quad (8)$$

The function $z(\zeta, \eta=0)$ for $|\zeta| \leq 1$ defines the curve AB in parametric form. From the definition of the functions u and w , an expression for the potential follows:

$$\varphi = -\frac{y^2}{2} + \text{Re} \int w(\zeta) \frac{dz}{d\zeta} d\zeta. \quad (9)$$

Singular integrals (8) and (9) can be calculated in terms of elementary functions. As a result, we obtain

$$\begin{aligned} \frac{z(\zeta)}{y_0} = \frac{1}{\pi} \left[\alpha^2 \left(\frac{y_m}{y_0} - 1 \right) - 1 \right] \ln \frac{\zeta - 1}{\zeta + 1} + \frac{\alpha^2(\alpha^2 - 1)}{\pi(\zeta^2 - \alpha^2)} \\ \times \left(\frac{y_m}{y_0} - 1 \right) \left(\ln \frac{\zeta - 1}{\zeta + 1} - \frac{\zeta}{\alpha} \ln \frac{\alpha - 1}{\alpha + 1} \right), \end{aligned} \quad (10)$$

$$\begin{aligned} \varphi = -\left(\frac{y}{y_0} - 1 \right)^2 + 2\alpha^2 \frac{y}{y_0} \left(\frac{y_m}{y_0} - 1 \right) \\ - \frac{1}{\pi} \text{Im} \left\{ \left[2\alpha^2 \left(\frac{y_m}{y_0} - 1 \right) + \alpha^4 \left(\frac{y_m}{y_0} - 1 \right)^2 - \frac{\alpha^4(\alpha^2 - 1)^2}{(\zeta^2 - \alpha^2)^2} \left(\frac{y_m}{y_0} - 1 \right)^2 \right] \ln \frac{\zeta - 1}{\zeta + 1} + (V_m - 1) \ln \frac{\alpha + \zeta}{\alpha - \zeta} \right. \\ \left. + \frac{\alpha(\alpha^2 - 1)\zeta}{\zeta^2 - \alpha^2} \left(\frac{y_m}{y_0} - 1 \right)^2 \left(\alpha - \frac{\alpha^2 - 1}{2} \ln \frac{\alpha - 1}{\alpha + 1} \right) + \frac{\alpha^3(\alpha^2 - 1)^2\zeta}{(\zeta^2 - \alpha^2)^2} \left(\frac{y_m}{y_0} - 1 \right)^2 \ln \frac{\alpha - 1}{\alpha + 1} \right\}. \end{aligned} \quad (11)$$

Expressions (10) and (11) in parametric form define the distribution of the potential $\varphi(x, y)$ in the depletion region. The first term describes the surface potential in the semiconductor in the absence of the contact, and the other terms describe the perturbation introduced by the contact. The unknown constants y_m and α should be found from the system of two equations

$$\frac{y_m}{y_0} - 1 = - \left[\frac{\pi a}{y_0} + 2 \ln \frac{\alpha - 1}{\alpha + 1} \right] / \left[2\alpha + (\alpha^2 + 1) \ln \frac{\alpha - 1}{\alpha + 1} \right], \quad (12)$$

$$\begin{aligned} \frac{1}{2} \left(\frac{y_m}{y_0} - 1 \right)^2 \left[\alpha^3 + \alpha + \frac{(\alpha^2 - 1)^2}{2} \ln \frac{\alpha - 1}{\alpha + 1} \right] \\ + 2\alpha \left(\frac{y_m}{y_0} - 1 \right) + 1 - V_m = 0, \end{aligned} \quad (13)$$

which follows from the boundary conditions for the potential and correspondence between the points of the complex planes z and ζ .

Figure 3 shows the dependences of the depletion thickness y_m under the metal on the voltage V applied to a contact for different contact sizes a . The curves were constructed using the system of Eqs. (12) and (13). Hereafter, it is assumed that for a zero voltage, the band bending is constant along the entire surface of the semiconductor; hence,

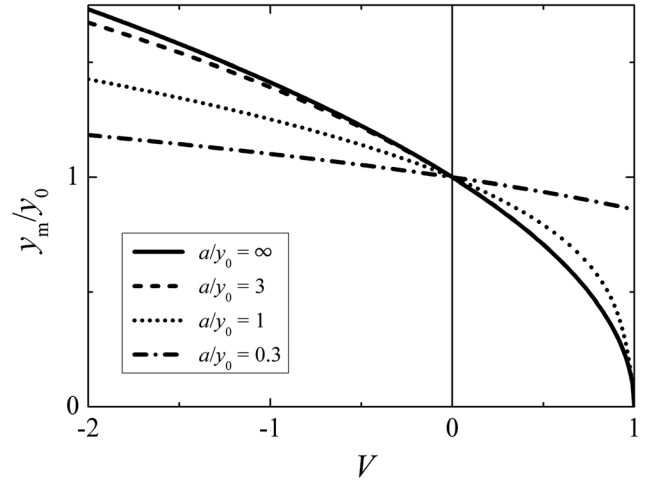


FIG. 3. Dependences of the depletion region thickness under the metal on applied bias for contacts of different lengths.

$V_m = 1 - V$. The dependence for $a = \infty$ corresponds to the one-dimensional model of the Schottky contact. The dependences become weaker with decreasing size of the contact.

Figure 4 shows the shapes of the boundaries of the depletion regions for contacts with the sizes $a = 3y_0$ (solid lines) and $a = 0.3y_0$ (dotted lines) under forward ($V = 0.5$) and backward ($V = -2$) biases. Arrows on the abscissa axis indicate the contact edges.

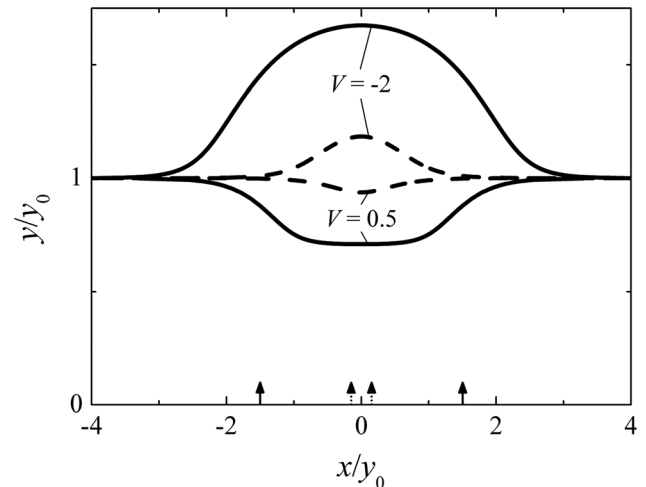


FIG. 4. Shapes of the boundaries of the depletion regions for contacts with the sizes $a = 3y_0$ (solid lines) and $a = 0.3y_0$ (dotted lines) under forward ($V = 0.5$) and backward ($V = -2$) biases. Arrows on the abscissa axis indicate the contact edges.

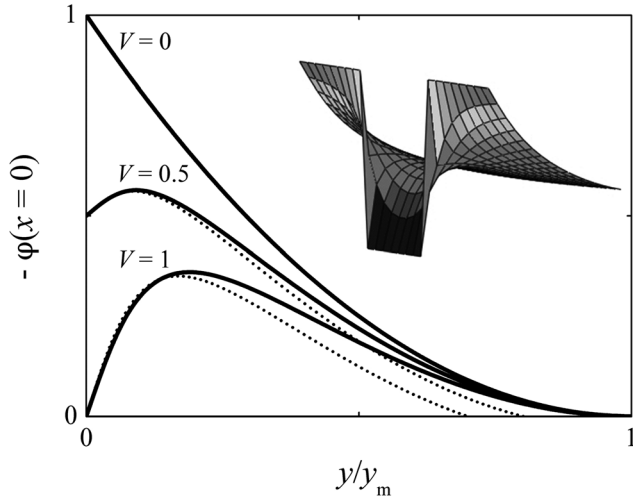


FIG. 5. Shapes of the potential barrier in the Schottky contact ($a=0.2y_0$) along the Oy axis for three forward biases V , namely, 0, 0.5, and 1. Dotted lines show the dependences constructed using an approximate theory from Ref. 7. The inset shows the saddle shape of the potential barrier, which appears in the semiconductor near the metal contact of small length under forward bias.

lines) and $a=0.3y_0$ (dotted lines) under forward ($V=0.5$) and backward ($V=-2$) biases. The curves were constructed using expression (10) and the system of Eqs. (12) and (13). Arrows on the abscissa axis indicate the edges of the contacts. The contact of small length depletes the semiconductor much weaker than the longer one.

In contacts of small length, the edge effects may lead to the occurrence of a saddle region of the potential distribution under forward biases. The inset of Fig. 5 shows schematically the position of the saddle region at the bottom of the conduction band in the semiconductor near the metal contact for this case. Figure 5 shows the behavior of the potential in the Schottky contact along the Oy axis at $a=0.2y_0$ for three different forward biases V , namely, 0, 0.5, and 1. Even for the voltage $V=1$, which in the one-dimensional model corresponds to the band flattening, a considerable potential barrier for electrons remains in the nanocontact. Solid curves were constructed using expressions (10)–(13). Dotted curves show the dependences plotted with an approximate theory from Ref. 7. It should be noted that the resulting solution can be used to describe the inhomogeneous Schottky contacts of stripe geometry containing the regions with modified barrier height.^{7,16}

III. HIGH-FREQUENCY CAPACITANCE OF THE SCHOTTKY CONTACT

Consider the behavior of the contact capacitance. In the model we used, the capacitance, generally speaking, is equal to the infinity since there are surface states of infinite density at the semiconductor boundary, which provides a gap of the boundary value of the potential at the edge of a metal layer. Therefore, a finite change in the metal layer potential leads to an infinitely large change in the charge of the surface states. This difficulty can be overcome in the further analysis of the problem by paying attention to the fact that the typical recharge time of electronic states on the free surface of a semiconductor is usually quite long.¹⁷ We consider the

capacitance of the Schottky contact at a frequency much greater than the rate of recharge of the surface states. In this case, the charge of the free surface of a semiconductor can be considered constant.

Let an infinitesimal high-frequency voltage δV_m be applied to the contact. This leads to a modulation of the position of the boundary of the depletion region of the semiconductor. In this case, the charge of the depletion region changes by δQ . The charge δQ is distributed in an infinitely thin layer of the semiconductor along the boundary of the depletion region. A charge of the same magnitude and opposite in sign is distributed along the metal surface. Distribution of the high-frequency potential $\delta\phi$ in the depletion region is described by Laplace's equation with the boundary conditions

$$(\delta\phi)_{AB} = 0, \quad (14)$$

$$(\delta\phi)_{DF} = \delta V_m, \quad (15)$$

$$\left(\frac{\partial\delta\phi}{\partial n}\right)_{B'D} = \left(\frac{\partial\delta\phi}{\partial n}\right)_{FA'} = 0, \quad (16)$$

$$(\nabla\delta\phi)_{x\rightarrow\pm\infty} = 0. \quad (17)$$

Boundary condition (16) is approximate. The approximation is good for $\varepsilon \gg 1$, which is true for most semiconductors.

To solve the boundary-value problem, we pass to the complex plane ζ . We introduce an analytical function f_1 , whose real part is the function $\delta\phi$, and consider the function $f = df_1/d\zeta = \partial\delta\phi/\partial\zeta - i\partial\delta\phi/\partial\eta$. From boundary conditions (14)–(17), it follows that $\text{Re } f = 0$ on the segments $(-\infty, -\alpha)$, $(-1, 1)$, and $(\alpha, +\infty)$ of the real axis and $\text{Im } f = 0$ on the segments $(-\alpha, -1)$ and $(1, \alpha)$. Thus, in the complex plane ζ , we pose a mixed boundary-value problem of finding the function f , which is analytical in the upper half-plane, from given values of its real and imaginary parts on the segments of the real axis. The solution of this problem is known.¹⁴ The solution that is symmetric with respect to the imaginary axis and belongs to the class of functions with bounded integral at infinity has the form

$$f(\zeta) = \frac{iA_0}{\sqrt{(\zeta^2 - 1)(\zeta^2 - \alpha^2)}}, \quad (18)$$

where A_0 is the real-valued constant. The high-frequency potential is found by integrating the function f in the complex plane ζ and taking the real part. The unknown constant A_0 is determined from the expression

$$\delta V_m = -A_0 \int_0^\infty \frac{d\eta}{\sqrt{(\eta^2 + 1)(\eta^2 + \alpha^2)}}, \quad (19)$$

which follows from boundary conditions (14) and (15). To find the charge δQ , we integrate the normal component of the electric field along the boundary with the metal. As a result, we obtain

$$\delta Q = -2A_0 \int_\alpha^\infty \frac{d\zeta}{\sqrt{(\zeta^2 - 1)(\zeta^2 - \alpha^2)}}. \quad (20)$$

Using expressions (19) and (20), we find the capacitance of the Schottky contact per unit length along the direction perpendicular to the xOy plane

$$C = \frac{\delta Q}{\delta V_m} = 2 \frac{K(1/\alpha)}{K(\sqrt{1-1/\alpha^2})}, \quad (21)$$

where K is the complete elliptic integral of the first kind. Dimensional and dimensionless capacitances are related by $\tilde{C} = \epsilon\epsilon_0 C$. The dependence of the parameter α on the static voltage V is found from the solution of system (12) and (13).

For $V=0$, the boundary with the quasi-neutral region is flat; therefore, in this case, the expression for the capacitance, which follows from Eqs. (12), (13), and (21), coincides with expression (19) from Ref. 18, which describes the capacitance between the infinite stripe and the parallel plane. The inset of Fig. 6 shows the dependences of the capacitance on the contact size at zero voltage, which were obtained in two- and one-dimensional models of the Schottky contact. Unlike the one-dimensional model, in which the capacitance linearly decreases, the two-dimensional capacitance decreases logarithmically when the contact size tends to zero. When the contact size tends to infinity, the capacitance in the two-dimensional model is different from the one-dimensional capacitance because of the edge effects. In the limiting cases, where the contact size is much less than or much greater than the thickness of the depletion region, expressions (12), (13), and (21) can be simplified, and the capacitance can be expressed in terms of elementary functions.

For $a \rightarrow 0$, the capacitance $C = \pi/\ln\left(\frac{16y_0}{\pi a} - \frac{4}{3}V\right)$. For $a \rightarrow \infty$, we have $C = \frac{a}{y_0\sqrt{1-V}} + \frac{2}{\pi}\left(2\ln 2 + 1 - \frac{1}{\sqrt{1-V}}\right)$, where the first term is the one-dimensional capacitance and the second term is the correction due to edge effects. The dependences of the capacitance on voltage for different contact sizes, which were constructed using Eqs. (12), (13), and (21), are shown in Fig. 6. The capacitance is normalized to its value at zero voltage. As the contact size is decreased to a value

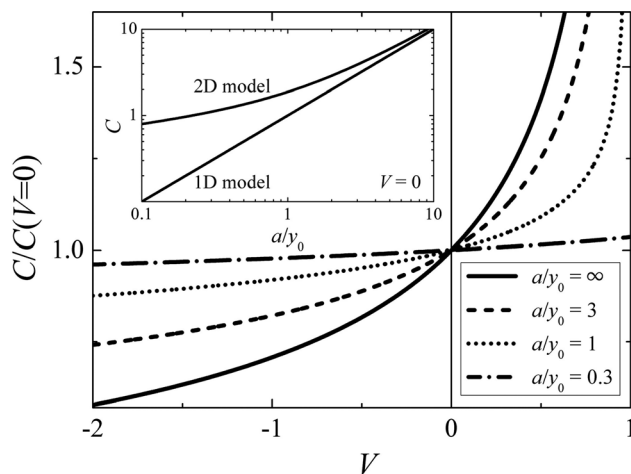


FIG. 6. Dependences of the capacitance on voltage for different lengths of the contact. The inset shows the dependences of the capacitance on the contact length at zero voltage, which was obtained in the one- and two-dimensional models of the Schottky contact.

severalfold less than y_0 , the capacitance virtually becomes uncontrolled by a constant voltage.

IV. SIGNAL DETECTION ANALYSIS IN THE FET WITH A SCHOTTKY BARRIER

There have recently been many papers devoted to the use of various types of FETs as nonresonant detectors of terahertz signals.^{19–21} The need for a simple uncooled sensing element operated in the mode of a zero applied direct current is related with the development of multiple systems of radiovision²² and other applications.²³ The principle of operation of the transistor in the detection mode is that the high-frequency voltage between the gate and the channel modulates a high-frequency current in the channel, resulting in that a constant component of the voltage appears between the source and drain. When optimizing the detector operation to reduce thermal noise, it is necessary to decrease the channel length of the transistor.²⁰ When the gate length is comparable with the distance between the gate and the channel, there appear the so-called short-channel effects associated with the two-dimensional distribution of the electric field under the gate. The analytical approach described in Secs. II–III permits one to consider these effects in terms of a simple model of the Schottky-barrier FET operated in the quadratic detection mode under a zero constant bias between the source and the drain.

Consider a transistor with the gate length a and the channel length d . Under a zero constant bias V_G between the channel and the gate, the thickness of the conductive part of the channel is l . The geometry of the transistor is shown in the inset of Fig. 7. Let low high-frequency voltages $\delta V_G = u_G \cos \omega t$ and $\delta V_D = u_D \cos(\omega t + \psi)$ be applied to the gate and the drain. A high-frequency current flows in the channel, the high-frequency potential changes along the AB boundary of the depletion region, and the tangential component of the electric field is not equal to zero. We now turn to the complex plane ζ . Now, unlike Sec. III, on segment $(-1, 1)$ of the real axis, we have $(\text{Re} f)_{\eta=0} = \left(\frac{\partial \delta \varphi}{\partial \zeta}\right)_{\eta=0} \neq 0$, and it is needed to define another boundary condition. If the

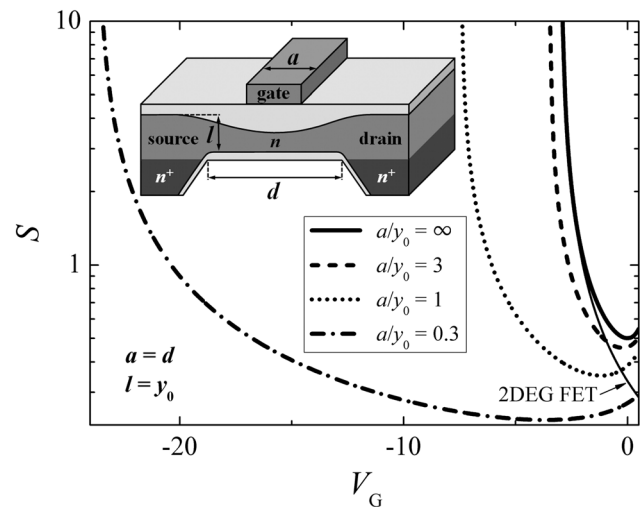


FIG. 7. Dependences of the quadratic nonlinearity parameter on the constant voltage between the gate and the channel for different lengths of the gate. The inset shows the geometry of the FET with a Schottky barrier.

boundary condition is specified; then, the solution of the boundary-value problem has the form¹⁴

$$f(\zeta) = \frac{i}{\sqrt{(\zeta^2 - 1)(\zeta^2 - \alpha^2)}} \times \left(A_1 - \frac{1}{\pi} \int_{-1}^{+1} \frac{(\partial \delta \varphi / \partial \zeta)_{\eta=0} \sqrt{(1 - \zeta^2)(\alpha^2 - \zeta^2)}}{\zeta - \zeta} d\zeta \right), \quad (22)$$

where A_1 is the real-valued constant. After this, as in Sec. III, we seek the high-frequency potential and determine A_1 from the boundary conditions.

$$\left(\frac{\partial \delta \varphi}{\partial \zeta} \right)_{\eta=0} = \begin{cases} -\delta V_D \frac{|dz/d\zeta|_{\eta=0}}{l + y_0 - y(\zeta)} \left(\int_{\xi(d/2)}^{\xi(-d/2)} \frac{|dz/d\zeta|_{\eta=0}}{l + y_0 - y(\zeta)} d\zeta \right)^{-1}, & \zeta \in (\xi(d/2), \xi(-d/2)) \\ 0, & \zeta \in (-1, \xi(d/2)) \cup (\xi(-d/2), 1) \end{cases} \quad (23)$$

Solving the boundary-value problem with this boundary condition, we find the modulation of the channel thickness, $\delta y(\zeta) = \frac{\text{Im} f(\zeta, \eta=0)}{|dz/d\zeta|_{\eta=0}}$, and the modulation of the channel conductivity, $\delta G_{\text{Ch}}/G_{\text{Ch}}$, by high-frequency voltage. Averaging the channel current over time, we find the constant component of the voltage between the source and the drain, which is the output signal of the detector

$$\Delta V = \frac{\langle \delta V_D \delta G_{\text{Ch}} \rangle}{G_{\text{Ch}}} = \frac{1}{2} \left(u_G u_D \cos \psi - \frac{1}{2} u_D^2 \right) S, \quad (24)$$

where

$$S = \int_{\xi(d/2)}^{\xi(-d/2)} \frac{(l + y_0 - y(\zeta))^{-2} d\zeta}{\sqrt{(1 - \zeta^2)(\alpha^2 - \zeta^2)}} \times \left(\int_0^\infty \frac{d\eta}{\sqrt{(\eta^2 + 1)(\eta^2 + \alpha^2)}} \int_{\xi(d/2)}^{\xi(-d/2)} \frac{|dz/d\zeta|_{\eta=0} d\zeta}{l + y_0 - y(\zeta)} \right)^{-1}. \quad (25)$$

Parameter S characterizes the quadratic nonlinearity of the transistor during detection. Dimensional and dimensionless parameters of the nonlinearity are related by $\tilde{S} = S/\tilde{V}_c$.

Figure 7 shows the dependences of the nonlinearity parameter of the constant gate voltage for different gate lengths at $a = d$ and $l = y_0$. The dependence for $a = \infty$ was constructed using the expression $S_{\text{ID}}^{\text{MESFET}} = \frac{1}{2\sqrt{1-V_{\text{th}}}(\sqrt{1-V_{\text{th}}}-\sqrt{1-V_{\text{G}}})}$

$\frac{\sqrt{1-V_{\text{th}}}-1}{(d/a-1)(\sqrt{1-V_{\text{th}}}-\sqrt{1-V_{\text{G}}})+\sqrt{1-V_{\text{th}}}-1}$, which can easily be obtained from a one-dimensional Schockley model of the field-effect transistor.²⁴ Here, V_{th} is the gate voltage at which the channel is shut off. For $a = d$, the second factor in this expression is equal to unity, and the condition $l = y_0$ corresponds to

In a simple model, we assume that the high-frequency current is uniformly distributed over the channel cross section, and is equal to zero in the regions of the source and the drain. We also assume that the channel conductivity is much greater than the conductivity between the channel and the gate, i.e., $G_{\text{Ch}} \gg \omega C_{\text{G}}$. Then, the tangential component of the electric field at the boundary AB is proportional to the current density in the channel, and it can be expressed in terms of the conductivity and cross section of the channel. In the case of symmetric arrangement of the gate in the middle of the channel, in the first order in high-frequency voltage, we obtain the following boundary condition:

$V_{\text{th}} = -3$. For comparison, by a faint line we show a similar dependence for the FET with a two-dimensional channel, $S_{\text{ID}}^{\text{2DEG FET}} = \frac{1}{V_{\text{G}} - V_{\text{th}}}$,²⁰ with the same V_{th} . The remaining curves were constructed using expression (25). With decreasing length of the gate, the dependences of the depletion thickness on the constant and high-frequency voltages between the gate and the channel become weaker. Therefore, the channel shut-off voltage increases and the nonlinearity parameter decreases.

Figure 8 demonstrates the influence of the channel part, which is inside the gate. This figure shows the dependences of the nonlinearity parameter on the constant voltage at the gate in the one- and two-dimensional models for $a = l = y_0$, in cases, where the channel and the gate are of equal length,

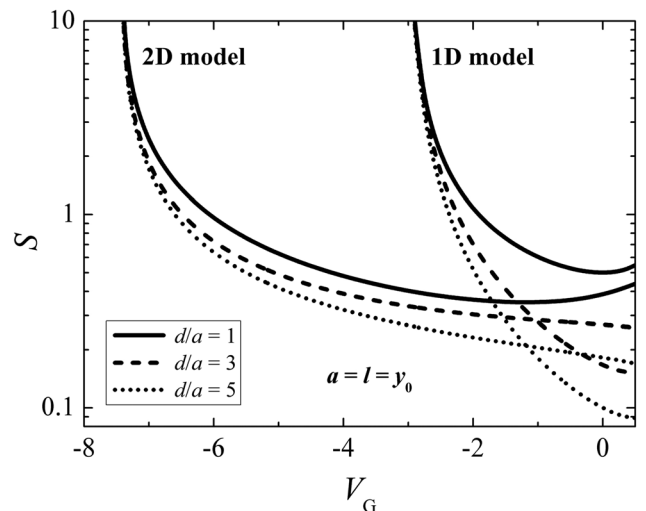


FIG. 8. Dependences of the quadratic nonlinearity parameter on the voltage between the gate and the channel in the one- and two-dimensional models for three cases, where the channel and the gate are of equal length, the channel is a factor of three longer than the gate, and the channel is a factor of five longer than the gate.

the channel is a factor of three longer than the gate, and the channel is a factor of five longer than the gate. In the one-dimensional model, the constant voltage at the gate controls the channel thickness only under the gate. The two-dimensional model allows for the influence of the gate voltage on the shape of the entire channel. This leads to a smaller difference between the dependences, which correspond to the channels of different lengths, in the two-dimensional model.

It should be noted that the above description of the transistor based on the full depletion approximation is adequate if the thickness of the conductive part of the channel is much larger than the Debye length. In the model, we used the nonlinearity parameter becomes infinite when the channel is shut off.

V. CONCLUSIONS

We have considered the model of a planar stripe Schottky contact to a semi-infinite, uniformly doped semiconductor. It was assumed that the position of the Fermi level at the boundary of the semiconductor is fixed due to the high density of surface states in the band gap. An exact analytical solution for the electrostatic potential distribution and the shape of the depletion region of the Schottky contact with an arbitrary stripe width is obtained in the full depletion approximation. The behavior of the high-frequency capacitance of the contact and quadratic nonlinear properties of the FET with a Schottky barrier in the detection mode have been studied. The results correctly describe a number of effects that cannot be obtained in the one-dimensional model. Among these effects, we mention the divergence of the electric field at the metal edges, the influence of the surface bending of the semiconductor bands outside the metal on the potential distribution and capacitance, significant weakening of the modulation of the depleted region thickness and capacitance by voltage with decreasing length of the contact, increase in the channel shut-off voltage, and decrease in the FET nonlinearity parameter with decreasing length of the gate. The solution is crucial for the description of contacts, whose length is less than or about the depletion thickness. For example, for the contact with length equal to the depletion thickness at zero voltage, the calculation made in the one-dimensional model underestimates the capacitance by

about two times and overestimates the relative modulation of capacitance by voltage about fourfold. With the backward bias, the error increases. For the FET, whose gate length is comparable with the depletion thickness, calculation of the nonlinearity parameter in the one-dimensional model gives an error of tens of percent at zero gate bias. With increasing bias that shuts off the channel, the error increases dramatically.

ACKNOWLEDGMENTS

This work was supported by the programs of the Russian Academy of Sciences.

- ¹R. T. Tung, *Appl. Phys. Rev.* **1**, 011304 (2014).
- ²H. Palm, M. Arbes, and M. Schulz, *Phys. Rev. Lett.* **71**, 2224 (1993).
- ³E. Wasserstrom and J. McKenna, *Bell Syst. Tech. J.* **49**, 853 (1970).
- ⁴G. D. J. Smit, S. Rogge, and T. M. Klapwijk, *Appl. Phys. Lett.* **81**, 3852 (2002).
- ⁵T. Sato, S. Kasai, and H. Hasegawa, *Jpn. J. Appl. Phys., Part 1* **40**, 2021 (2001).
- ⁶J. P. Sullivan, R. T. Tung, M. R. Pinto, and W. R. Graham, *J. Appl. Phys.* **70**, 7403 (1991).
- ⁷R. T. Tang, *Appl. Phys. Lett.* **58**, 2821 (1991).
- ⁸G. Lengyel, P. Meissner, E. Patzak, and K.-H. Zschauer, *IEEE Trans. Microwave Theory Tech.* **30**, 464 (1982).
- ⁹W. R. Frensley, *IEEE Trans. Electron Devices* **28**, 962 (1981).
- ¹⁰A. Kloes, M. Weidemann, D. Goebel, and B. T. Bosworth, *IEEE Trans. Electron Devices* **55**, 3467 (2008).
- ¹¹T. Holtij, M. Graef, F. M. Hain, A. Kloes, and B. Iniguez, *IEEE Trans. Electron Devices* **61**, 288 (2014).
- ¹²J. Si, J. Wei, W. Chen, and B. Zhang, *IEEE Trans. Electron Devices* **60**, 3223 (2013).
- ¹³O. T. Gavrilov and I. I. Kvyatkevich, *Elektron. Tekh., Ser. 2* **7**(158), 3 (1982) (in Russian).
- ¹⁴F. D. Gahov, *Boundary Value Problems* (Pergamon Press, Oxford, 1966).
- ¹⁵L. V. Ahlfors, *Complex Analysis* (McGraw-Hill, New York, 1979).
- ¹⁶R. T. Tung, *Phys. Rev. B* **45**, 13509 (1992).
- ¹⁷S. M. Sze and K. K. Ng, *Physics of Semiconductor Devices* (Wiley Interscience, Hoboken, 2007).
- ¹⁸B. Gelmont, M. S. Shur, and R. J. Mattauch, *Solid-State Electron* **38**, 731 (1995).
- ¹⁹M. Sakowicz, M. B. Lifshits, O. A. Klimenko, F. Schuster, D. Coquillat, F. Teppe, and W. Knap, *J. Appl. Phys.* **110**, 054512 (2011).
- ²⁰S. Preu, S. Kim, R. Verma, P. G. Burke, M. S. Sherwin, and A. C. Gossard, *J. Appl. Phys.* **111**, 024502 (2012).
- ²¹M. Sakhno, A. Golenkov, and F. Sizov, *J. Appl. Phys.* **114**, 164503 (2013).
- ²²A. Rogalski and F. Sizov, *Opto-Electron. Rev.* **19**, 346 (2011).
- ²³E. R. Brown, *Int. J. High Speed Electron. Syst.* **13**, 995 (2003).
- ²⁴M. Shur, *GaAs Devices and Circuits* (Plenum Press, New York, 1987).